

Numerical Simulation of Pulsed Laser Transformation Hardening

Gang Yu^{*}, Wei Wu, Naigang Liang

DTS, Institute of Mechanics, Chinese Academy of Sciences, Beijing, 100080, China

e-mail: gyu@imech.ac.cn, wuwei@lnm.imech.ac.cn, lng@lnm.imech.ac.cn

Abstract A novel pulsed laser surface processing technology is introduced, which can make use of the spatial and temporal profile of laser pulse to obtain ideal hardening parameters. The intensity distribution of laser pulse is spatially and temporally controlled by using laser shape transformation technology. A 3D numerical model including multi-phase transformations is established to explore material microstructure evolution induced by temperature field evolution. The influences of laser spatial-temporal profiles on hardening parameters are investigated. Different from the continuous laser processing technology, results indicate that spatial and temporal profiles are important factors in determining processing quality during pulsed laser processing method.

Key words: laser transformation hardening, laser shape transformation, multi-phase transformation, spatial and temporal profile

INTRODUCTION

The discovery of laser in 1960 has captured enormous efforts for its application in various fields, especially in material processing. With the improvement of reliability and durability, lasers practically began to be applied in material cutting, welding and drilling by the early 1970s [1]. The development of high power lasers and automatic control technology boosted the future applications in material surface processing, such as heat treatment, cladding, alloying, glazing and texturing, etc.

Because of the unique advantages over traditional heat treatment methods, laser transformation hardening has attracted a great deal of attentions in many industrial fields. The method offers the chance to allow improved components with desired surfaces without affecting the bulk properties. Compared to the alternative processes, laser surface treatment has such virtues as chemical cleanliness, low thermal distortion, good controllability of beam shape, less post-treatment work, remote non-contact processing, and good adaptability to geometry of component, etc. [2]

The general method of laser transformation hardening mainly relied on a beam continuously scanning across the surface of material, therefore, models usually focused on the relationship of beam velocity and hardening parameters. In 1979, W. M. Steen and C. Courtney [2] investigated the transformation hardening of En8 steel using a 2kW CO₂ laser, and obtained an empirical relationship between hardened depth and laser parameters including power, beam diameter, as well as velocity. In 1983, S. Kou, D. K. Sun and Y. P. Le [3] developed a three-dimension heat flow model using the finite difference method and described a theoretical analysis and solid-state phase transformations during laser surface hardening of 1018 steel. In 1984, M. F. Ashby and K. E. Easterling [4] combined approximate solutions to the one-dimensional heat flow equations with kinetic models to investigate laser hardening of hypoeutectoid steels and produce laser processing diagrams. In 1991, H. R. Shercliff and M. F. Ashby [5] developed an approximate heat flow model to predict the case depth for Gaussian and uniform rectangular laser sources. R. Komanduri and Z. B. Hou [6] presented an analytical model that is applicable for both transient and quasi-steady state conditions, and obtained the temperature rise distribution of a steel workpiece with finite width using a disk heat source with pseudo-Gaussian heat intensity distribution. For a given depth of hardening, the authors also provided the relationship between inputted laser parameters. J. C. Li [7] introduced a

semi-analytic calculation model on acting between laser and material and discussed some quick calculation methods that closer to actual application and got the experimental support.

Recent years, with the development of laser integrated systems and laser shape transformation technology, a novel processing technique known as “dot matrix hardening” has been developed by using a pulsed laser, which makes use of the spatial and temporal profile of laser pulse to obtain ideal hardening parameters [8,9].

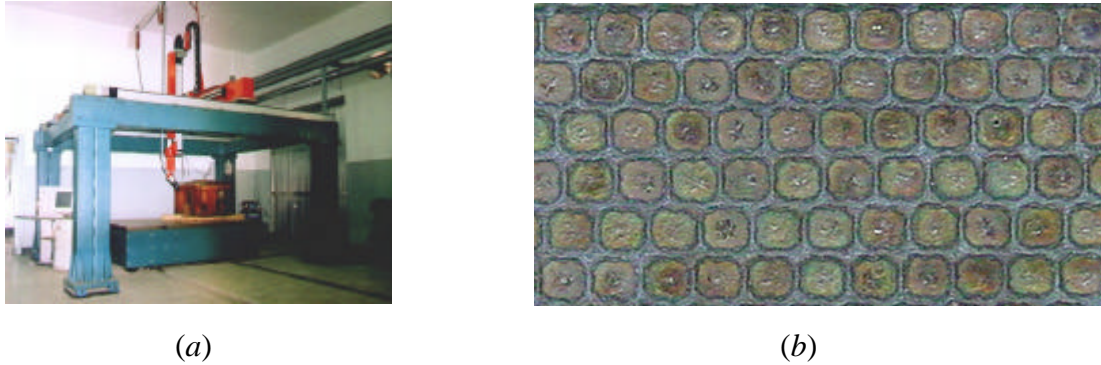


Fig. 1 Laser integrated systems (a) and hardened surface of material (b)

Fig. 1(a) displays the laser integrated robot system by which the raw laser pulse is spatially and temporally transformed into certain shape, then irradiate on material surface. With the discrete motion of laser, material surface is hardened spot by spot as shown in Fig. 1(b). In comparison with continuous laser surface hardening method, the discrete spot surface transformation hardening method is more suitable for the components with more complex surface shape such as automobile moulds etc., moreover, higher processing quality involving case depth, coverage rate and surface roughness, etc. can achieve by adjusting the spatial and temporal profile of laser beam through raster system.

Different from the most models for continuous laser transformation hardening, in which quasi-steady state behavior is typically assumed [8], models for pulsed laser transformation hardening should consider the transient phenomena and the the spatial-temporal profile of laser pulse. In present study, a 3D numerical model is established to explore the microstructure evolution during pulsed laser transformation hardening. In the model, laser spatial and temporal intensity distribution, temperature-dependent thermo-physical properties of material, and multi-phase transformations are considered. The influences of laser spatial pattern and temporal profile on microstructure evolution are investigated. The detailed descriptions of the model will be given in another report and only a brief presentation is presented here.

LASER MATERIAL INTERACTION

When a laser beam is incident on the surface of opaque material such as metal, in general, partial of the laser energy will be reflected and the other will be absorbed by the material. The absorbed laser will lead to the interaction between photons and bound as well as free electrons in the substrate material, which will result in these electrons to be raised to higher energy levels. The absorbed laser energy will change into heat energy through successive collisions between the excited electrons and the crystal lattice of material, i.e., relaxation process. In the relaxation process, the energy transport between the electrons and lattice site atoms is in a nonequilibrium state. However, the relaxation time for metal is of the order of 10^{-13} s [10] and the laser pulse in this study is 10^{-3} s, hence the Fourier’s law of heat conduction is still appropriate to describe the heating process. In addition, the absorption depth of laser is of the order of its wavelength [11], which, in general, is of the order of micron. For laser transformation hardening, the desired thickness of hardened layer is of the order of hundred microns, so the laser pulse can be considered plane heat source.

MICROSTRUCTURE EVOLUTION

At room temperature, generally speaking, steel is the mixture of ferrite and pearlite, and cast iron is the mixture of ferrite, pearlite, cementite and graphite. During a whole thermal cycle including heating and

cooling processes, the original microstructures will undergo a series of transformations according to different conditions.

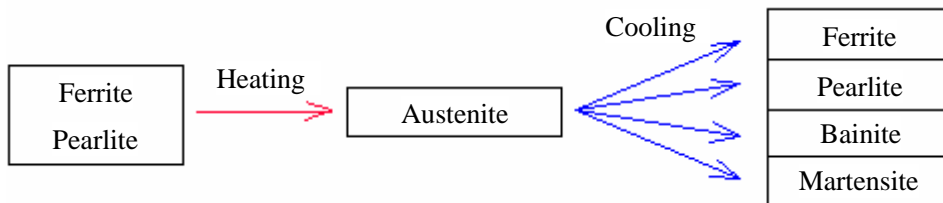


Fig. 2 Schematic diagram of the possible phase transformations during a whole thermal cycle

Fig. 2 illustrates the possible microstructure phase transformations of steel or cast iron. General speaking, the pearlite or ferrite will change into austenite during heating course and then transform into different microstructures according to different conditions during cooling course.

1. Heating course When suitable laser pulse acts on the surface of material, the local temperature will rapidly be in excess of austenizing critical temperature and below the melting point. In this heating course, the pearlite or ferrite will transform into austenite. The transformation of pearlite or ferrite to austenite is completed through carbon diffusion. For laser transformation hardening, temperature should remain above the austenizing critical temperature for a sufficient time for carbon diffusion, and the required time is estimated about 3ms [12].

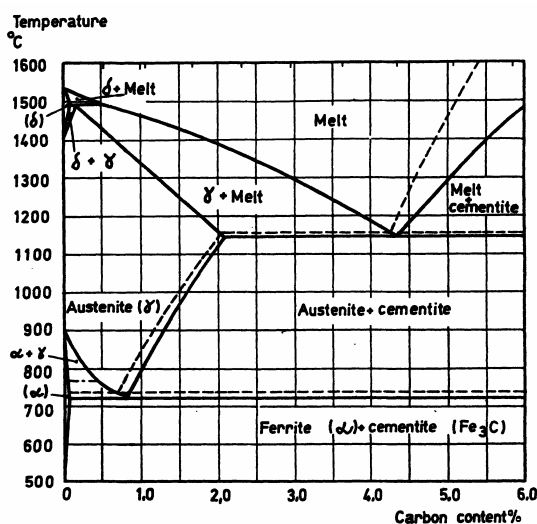


Fig. 3 Fe-C equilibrium diagram

The typical Fe-C equilibrium diagram is reproduced in Fig. 3 [13], from which the phase transformation information such as the critical point and temperature range, as well as transformation condition etc. can be obtained. It should be pointed out that the information given by equilibrium diagram are under the condition of equilibrium state. However, the heating rate is so rapid that phase transformations will occur in a non-equilibrium state during laser surface hardening, which will result in the basic diagram no longer valid in some cases. The high heating rate will cause a delay in the austenite transformation and consequently a shift in the transformation temperature [14].

2. Cooling course When laser pulse ceases to irradiate, the material will rapidly cool down due to the surrounding material acting as an efficient heat sink, which will result in the formation of hard martensite phase. The process is so-called “self-quenching”. Different from austenite phase transformation, carbon diffusion does not happen in the martensite formation, instead, each carbon atom maintains nearly the same location as it had in the austenite [15]. In fact, austenite will transform into different phases such as pearlite, bainite and martensite, etc. according to different cooling velocity. Fig. 4 is the sketch to describe the influence of the cooling rate on phase transformations. In the figure, v_1 and v_2 are lower and upper critical cooling rate respectively. In order to simplify the calculation, present model considers that austenite

will completely transform into pearlite if cooling rate is less than v_1 , and martensite if cooling rate is more than v_2 and temperature is below martensite critical temperature M_s . If the cooling rate is between v_1 and v_2 , austenite will partially transform into martensite when the temperature is below M_s .

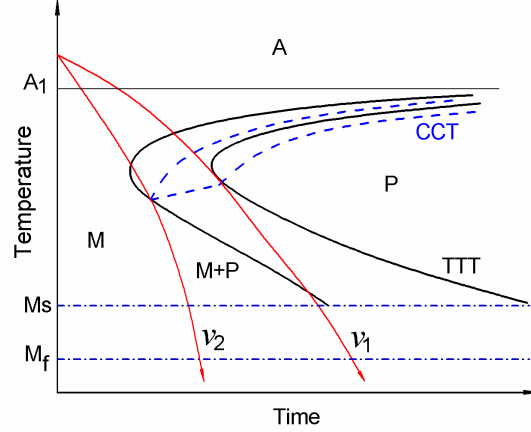


Fig. 4 Schematic diagram of phase transformation during cooling course

TEMPERATURE FIELD EVOLUTION

As mentioned above, the traditional Fourier's law of heat conduction is still available in describing current pulsed laser transformation hardening and the general type of heat conduction equation takes the form

$$\mathbf{r}c \frac{\partial T}{\partial t} = \nabla \cdot (k\nabla T) + \mathbf{r}\dot{Q} \quad (1)$$

where \mathbf{r} is the material density, c the specific heat, k the thermal conductivity, and \dot{Q} the rate of internal energy generation of per unit mass.

During laser processing, although heat energy losses duo to convection and radiation are unavoidable, researches [3, 7] indicated that these kind energy losses can be neglected, so the corresponding boundary conditions are specified temperature $T=T(\Gamma_1, t)$ on boundary Γ_1 and specified heat flow $q=q(\Gamma_2, t)$ on boundary Γ_2 , where $\Gamma_1 + \Gamma_2 = \Gamma_{\text{total}}$ (entire boundary). The initial condition is $T=T_0(x, y, z)$.

For most engineering materials such as steel and cast iron are not pure substances, phase transformation always occurs over a temperature range other than a discrete critical point, and so latent heat can be handled to be equivalent specific heat. When phase transformation takes place, the quantity of heat released or absorbed Q is the function of temperature T and in present study the linear assumption is adopted, therefore, according to Eq. (1), there have

$$\mathbf{r}c \frac{\partial T}{\partial t} = \nabla \cdot (k\nabla T) - \mathbf{r} \frac{\partial Q}{\partial t} \quad (2)$$

$$\mathbf{r}c \frac{\partial T}{\partial t} = \nabla \cdot (k\nabla T) - \mathbf{r} \frac{\partial Q}{\partial T} \frac{\partial T}{\partial t} \quad (3)$$

$$\mathbf{r}c \frac{\partial T}{\partial t} = \nabla \cdot (k\nabla T) - \mathbf{r}c_q \frac{\partial T}{\partial t} \quad (4)$$

$$\mathbf{r}(c + c_q) \frac{\partial T}{\partial t} = \nabla \cdot (k\nabla T) \quad (5)$$

$$\mathbf{r}\bar{c} \frac{\partial T}{\partial t} = \nabla \cdot (k\nabla T) \quad (6)$$

where $\bar{c} = c + c_q$ is called average specific heat, and c_q is the equivalent specific heat. Equation (6) is solved with finite element method in present study.

INFLUENCE OF LASER SPATIAL PATTERN

In present study, a ND:YAG laser with the wavelength of $1.06\mu\text{m}$ and per pulse energy of 11 Joules are adopted. The raw laser beam was spatially transformed into two types of pattern to investigate the influences on microstructure evolution. Fig. 5(a) and (b) show the geometric shape of point type pattern and mesh type pattern, respectively. For the two types of pattern, the effective area of laser pulse acting on is the same, and can be calculated by the parameters $a=1.12\text{mm}$, $b=0.72\text{mm}$ and $c=0.18\text{mm}$. The spatial intensity distribution of laser pulse is controlled to be uniform and the temporal profile is set to be rectangle with pulse duration 24ms. A kind of pearlitic ductile iron named QT50 that mainly contains 3.7% C and 2.6% Si by weight is selected to explore the influence of different laser spatial patterns on microstructure evolution. The related thermal-physics properties can be found in Refs. [16-19].

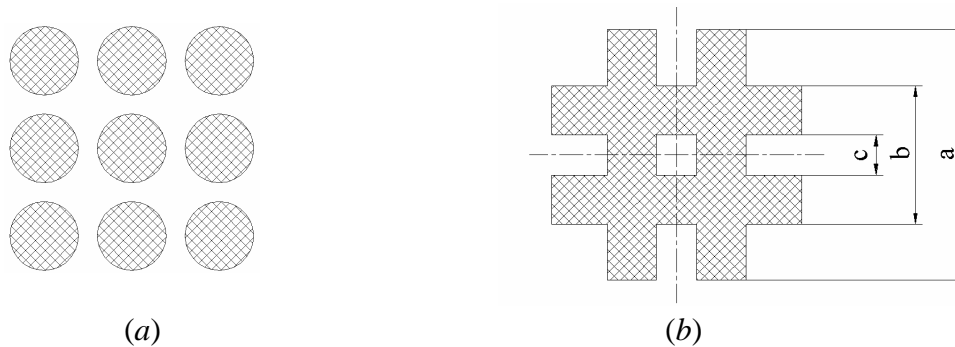


Fig. 5 Point type (a) and mesh type (b) patterns of laser pulse

8-node-hexahedron element is adopted in the 3D finite element analysis. Only 1/4 of the laser pattern and material piece are considered according to symmetry. Adiabatic boundary conditions are set on the symmetrical surfaces and the region no laser acting of the top surface. On the lateral surfaces, isothermal boundary conditions are given, i.e., temperature is specified. For the region laser acting on, heat flow is specified. The initial temperature is set to be room temperature 25°C . The mean value of surface absorption coefficient of present material to ND:YAG laser is about 0.20 to 0.25 according to our experiment. The hardened regions of the two different types of laser pattern are given in Fig. 6, in which (a) is the case of the point type and (b) the mesh type. From the figures, it can be seen that the geometric shapes are different. For case (a), the point type, the hardened depth is about 150mm and the surface maximum temperature is about 1250°C . For case (b), the mesh type, the hardened depth and surface maximum temperature are 180mm and 1310°C , respectively. Although the surface maximum temperature of case (b) is higher than that of case (a), it is below the melting point of the material $1250\sim 1350^{\circ}\text{C}$, which is required by laser transformation hardening. In general, the hardened depth is anticipated to be as deep as possible under certain power intensity during pulsed laser transformation hardening. From this point of view, certain laser spatial pattern should be selected. In present study, the mesh type pattern appears preferable to the point one.

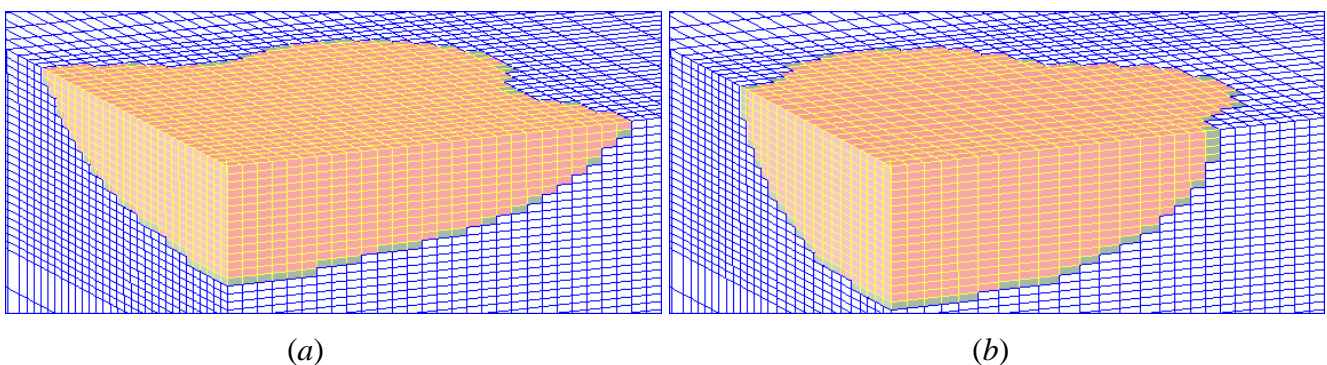


Fig. 6 The hardened regions of point type (a) and mesh type (b)

INFLUENCE OF LASER TEMPORAL PROFILE

In order to investigate the influence of laser temporal profiles on microstructure evolution, four different temporal profiles are chosen as shown in Fig. 7. In the figure, case (a) is called rectangle, case (b) forward-triangle, case (c) back-triangle, and case (d) double-triangle. In this study, mesh type shown in Fig. 5(b) of laser pulse spatial pattern is adopted. Laser pulse energy and duration t_0 are 11 Joules and 24ms, respectively. Apparently, the peak power intensity of cases (b), (c), (d) is the same and is twice of that of case (a). It should be pointed that the detailed discussions of the influences of temporal profiles are available on another report.

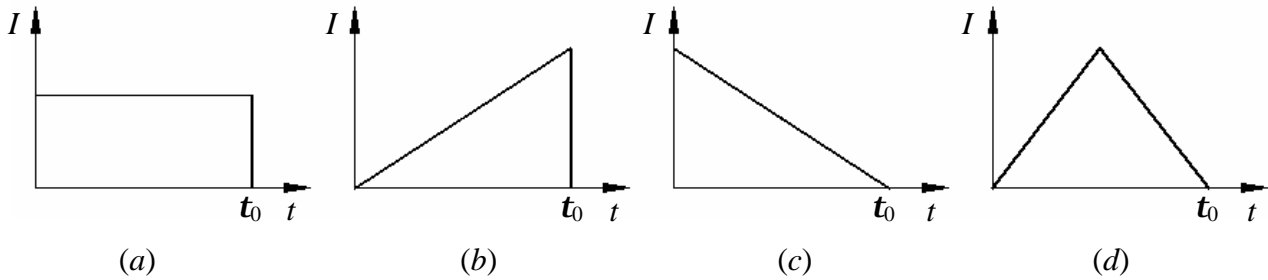


Fig. 7 Four temporal profiles

The geometric shapes of hardened region for the different four temporal profiles are similar to the shape shown in Fig. 6(b). The results of hardened depth and surface maximum temperature are shown in Table 1.

Table 1. Results for different temporal profiles

Temporal profile	(a)	(b)	(c)	(d)
Hardened depth (mm)	180	235	195	220
Surface maximum temperature (°C)	1310	1910	1440	1630

From the table, it can be seen that temporal profile (b) generates higher surface maximum temperature and deeper hardened layer than those of the other cases. Although the hardened depth of cases (b), (c) and (d) are all deeper than case (a), the surface maximum temperature of the former cases are all in excess of the melting point of material, which should be avoided during laser surface hardening. Obviously, when laser pulse energy is 11 Joules, temporal profile (a), rectangle shape, is more suitable than the others for obtaining desired hardening quality.

DISCUSSIONS

Deferent from continuous laser transformation hardening, in which beam velocity is often an important factor to be determined, the laser spatial pattern and temporal profile should be paid sufficient attention to during pulsed laser transformation hardening. When the other conditions are the same, different laser spatial patterns or temporal profiles will produce different hardening results.

Typical models for continuous laser transformation hardening often aimed to obtain quasi-steady state solutions, which can be quite useful for the cases where the laser beam diameter is large compared to the region of interest or the beam velocity is reasonably large. For the pulsed laser transformation hardening with a stationary laser pulse, the transient behavior should be taken into account [8]. Not only that, present model for pulsed laser surface hardening considers that the evolution of temperature field and microstructure together, instead of investigating the two kinds of evolution apartly and independently.

In fact, the microstructure evolution of material such as steel and cast iron is very complex during laser transformation hardening. The carbon diffusion and the influence of alloy elements such as Mn, Si, etc. are not yet considered in present study. The related work is being studied and we hope to report our progress on the further development of present model in the near future.

CONCLUSIONS

- 1) Pulsed laser transformation hardening is introduced, which can make use of the spatial pattern and temporal profile of laser pulse to obtain ideal hardening parameters.
- 2) A 3D numerical model for pulsed laser transformation hardening is established, in which laser spatial and temporal intensity distribution, temperature-dependent thermo-physical properties of material, and multi-phase transformations are considered.
- 3) Laser shape transformation technology is conducted to acquire certain laser spatial pattern.
- 4) The influences of laser spatial patterns and temporal profiles on microstructure evolution of a kind of ductile iron are investigated. In order to obtain desired hardening quality, certain spatial pattern and temporal profile of laser pulse should be selected.

Acknowledgements This research work was sponsored by Chinese Academy of Sciences through Grant KGCX1-11, National Natural Science Foundation of China through Grant No. 10232050, and also partly by Ministry of Science and Technology Foundation No. 2002CB412706.

REFERENCES

- [1] J. F. Ready, *Industrial applications of lasers*, Academic Press, New York, (1978).
- [2] W. M. Steen, *Laser material processing*, Springer-Verlag, London, (1991).
- [3] S. Kou, D. K. Sun, Y. P. Le, *A fundamental study of laser transformation hardening*, Metall. Trans. A, 14A, (1983), 643-653.
- [4] M. F. Ashby, K. E. Easterling, *The transformation hardening of steel surfaces by laser beams—I. hypo-eutectoid steels*, Acta Metall., 32, (1984), 1935-1948.
- [5] H. R. Shercliff, M. F. Ashby, *The prediction of case depth in laser transformation hardening*, Metallurgical Transactions A, 22A, (1991), 2459-2466.
- [6] R. Komanduri, Z. B. Hou, *Thermal analysis of the laser surface transformation hardening process*, Int. J. Heat Mass Transfer, 44, (2001), 2845-2862.
- [7] J. C. Li, *Diffraction of laser and calculation on thermal acting*, Science Press, Beijing, (2002).
- [8] P. R. Woodard, J. Dryden, *Thermal analysis of a laser pulse for discrete spot surface transformation hardening*, J. Appl. Phys., 85, (1999), 2488-2496.
- [9] G. Yu, H. J. Yu, *Integrated laser intelligent manufacturing*, Metallurgic Industry Press, Beijing, (2002).
- [10] M. von Allmen, *Laser-beam interactions with materials—physical principles and applications*, Springer-Verlag Berlin Heidelberg, Germany, (1987).
- [11] L. Migliore, *Laser – material interactions*, in L. Migliore ed. *Laser materials processing*, Marcel Dekker, Inc., New York, (1996).
- [12] M. Davis, P. Kapadia, J. Dowden, et al, *Heat hardening of metal surfaces with a scanning laser beam*, J. Phys. D, 19, (1986), 1981-1997.
- [13] K. E. Thelning, *Steel and its heat treatment*, Butterworth & Co (Publishers) Ltd, London, (1975).
- [14] J. C. Ion, H. R. Shercliff, M. F. Ashby, *Diagrams for laser materials processing*, Acta Metall. Mater., 40, (1992), 1539-1551.
- [15] C. R. Brooks, *Heat treatment of ferrous alloys*, Hemisphere Pub. Corp., Washington, (1979).
- [16] Y. Q. Liu, *Heat treatment of steel*, Metallurgic Industry Press, Beijing, (1987).
- [17] Z. Tan, G. W. Guo, *Thermophysical properties of engineering alloys*, Metallurgic Industry Press, Beijing, (1994).
- [18] Z. Z. Hu, *Handbook of steels and heat treatment curves*, National Defence Industry Press, Beijing, (1986).
- [19] Z. G. Zhao, L. W. Zhang, Z. B. Zhang, et al, *Calculation of temperature field of MoCu nodular cast iron in laser quenching process*, J. of Dalian University of Technology, 35, (1995), 164-169.